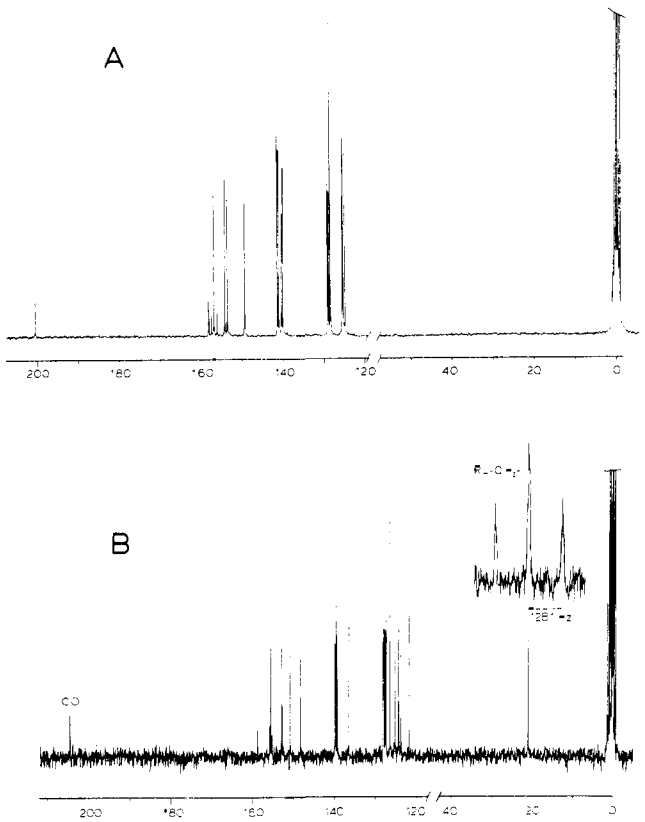

Figure 2. $^{13}C\{^1H\}$ NMR spectrum in CD_3CN of (a) *cis*-$[Ru(bpy)_2(CO)Cl]^+$ produced by the reaction between PhC≡CH and *cis*-$Ru(bpy)_2Cl_2$ and (b) *cis*-$[Ru(bpy)_2(CO)(\eta\text{-}CH_2Ph)]^+$ produced by the reaction between PhC≡CH and *cis*-$[Ru(bpy)_2(H_2O)_2]^{2+}$. The nitrile carbon resonance of CD_3CN has been deleted for clarity.

H_3PO_4) compared with −6.0 and −20.1 ppm for PPh_3 and *trans*-$[Ru(trpy)(PPh_3)_2Cl]^+$, respectively.[12] It can be inferred from the chemical shift data that PPh_3 is trans to a powerful electron-donating substituent.

Further indication that the benzyl group is a powerful σ donor at Ru^{II} comes from cyclic voltammetry and electronic spectral data. In acetonitrile, oxidation of Ru(II) to Ru(III) for *cis*-$[Ru(bpy)_2(CO)(\eta\text{-}CH_2Ph)]^+$ is shifted negatively by ca. 0.7 V ($E_{p,a}$ = 0.76 V vs. SCE) compared to *cis*-$[Ru(bpy)_2(CO)Cl]^+$ ($E_{1/2}$ = 1.50 V). The λ_{max} for the lowest $\pi^*(bpy) \leftarrow d\pi(Ru)$ CT transition in CH_3CN, which is also a measure of electron density[8] at Ru^{II}, is at 476 nm for *cis*-$[Ru(bpy)_2(CO)(\eta\text{-}CH_2Ph)]^+$ and at 400 nm (sh) for *cis*-$[Ru(bpy)_2(CO)Cl]^+$.

The mechanism(s) for the conversion of phenylacetylene to CO and toluene or to CO and the benzyl complex are not known in detail but are currently under investigation. Reasonable intermediates that can be anticipated are acetylene, vinylidene, acetylide, hydroxycarbene, and acyl complexes, all of which have chemical precedents in the chemistries of Re^I, Pt^{II}, Ru^{II}, or Fe^{II}.[15] The chemistry appears to be general for terminal alkynes in that we have also observed reactions with acetylene and 1-hexyne, and it seems clear that we will be able to study the mechanisms of the reactions in some detail.

Acknowledgment. We thank Ron Cerny for mass spectral measurements, Dr. David Harris for NMR spectroscopy experiments, Dr. Joe Templeton for his time and advice, and the National Science Foundation under Grant No. CHE-8008922 for support of this research.

Registry No. PhC≡CH, 536-74-3; *cis*-$Ru^{II}(bpy)_2Cl_2$, 19542-80-4; *cis*-$[Ru^{II}(bpy)_2(H_2O)Cl]^+$, 76739-35-0; $PhCH_3$, 108-88-3; *cis*-$[Ru^{II}(bpy)_2(CO)Cl](PF_6)$, 79850-20-7; *cis*-$[Ru^{II}(bpy)_2(H_2O)_2]^{2+}$, 72174-09-5; *trans*-$[Ru^{II}(bpy)_2(H_2O)_2]^{2+}$, 72174-10-8; *cis*-$[Ru^{II}(bpy)_2(CO)(\eta\text{-}CH_2Ph)](PF_6)$, 82482-60-8; *cis*-$[Ru^{II}(trpy)(PPh_3)(H_2O)_2]^{2+}$, 82482-61-9; *cis*-$[Ru^{II}(bpy)_2(CO)(\eta\text{-}CH_2Ph)]^+$, 82482-59-5; $[Ru^{II}(trpy)(PPh_3)(CO)(\eta\text{-}CH_2Ph]^+$, 82482-62-0; $Ru^{II}(bpy)_2CO_3$, 59460-48-9.

(15) (a) Chisholm, M. H.; Clark, H. C. *Acc. Chem. Res.* **1973**, *6*, 202. (b) Bates, D. J.; Rosenblum, M.; Samuels, S. B.; *J. Organomet. Chem.* **1981**, *209*, C55. (c) Jolly, P. W.; Pettit, R. *Ibid.* **1968**, *12*, 491. (d) Green, M. L. H.; Hurley, C. R. *Ibid.* **1967**, *10*, 188. (e) Kolobna, N. E.; Antova, A. B.; Khitrova, O. M.; Artipin, M. Y.; Struchkov, Y. T. *Ibid.* **1977**, *137*, 67 and references therein. (f) Belleby, J. M.; Mays, M. J. *Ibid.* **1976**, *117*, C21. (g) Treichel, P. M.; Komar, D. A. *Inorg. Chim. Acta* **1980**, *42*, 277. (h) Davison, A.; Seleque, J. P. *J. Am. Chem. Soc.* **1978**, *100*, 7763. (i) Bruce, M. I.; Wallis, R. C. *Aust. J. Chem.* **1979**, *32*, 1471.

Iron EXAFS of the Iron–Molybdenum Cofactor of Nitrogenase

Mark R. Antonio,[1a] Boon-Keng Teo,*[1b]
W. H. Orme-Johnson,[1c]* Mark J. Nelson,[1c] Susan E. Groh,[1c]
Paul A. Lindahl,[1c] Susan M. Kauzlarich,[1a] and
Bruce A. Averill*[1b]

Department of Chemistry, Michigan State University
East Lansing, Michigan 48824
Bell Laboratories, Murray Hill, New Jersey 07974
Department of Chemistry
Massachusetts Institute of Technology
Cambridge, Massachusetts 02139
Received February 1, 1982

Chemical and physical analyses indicate that the iron–molybdenum cofactor (FeMo(co)) of nitrogenase contains 6–8 mol of iron and 4–6 mol of sulfur per mol of molybdenum.[2-5] The physical properties of this cofactor suggest that it contains a novel Mo–Fe–S cluster.[4] The complementation of inactive molybdenum–iron protein by isolated cofactor[2,3] indicates that it is an important functional component of the enzyme. Thus, determination of the structure of the cofactor is of significance and interest.

Extended X-ray absorption fine structure (EXAFS) data taken at the Mo edge indicate that the molybdenum has two or three iron atoms and four or five sulfur atoms as nearest neighbors.[6-8] Several models are consistent with these data, including those with (1) a $MoFe_3S_4$ cluster with one molybdenum and three iron atoms at alternate corners of a distorted cube,[9,10] (2) two Fe atoms bridged by a MoS_4 group,[6] (3) two Fe_4S_4 cubes bridged by a MoS_4 unit,[8] (4) two Fe_3S_3 units bridged by a molybdenum atom,[11] and (5) a $[L_3MoFe_7S_6(SR)_7]^{z-}$ cluster containing a $MoFe_7S_6$ core with the metal atoms situated at corners of a cube and the quadruply bridging sulfurs occupying the six faces of the cube.[12] More information concerning the iron environment is needed to define the structure of the FeMo(co). We report here the successful measurement and analysis of the iron edge EXAFS of the FeMoco from *Azotobacter vinelandii* and relate initial structural information about the iron sites in that cluster.

(1) (a) Department of Chemistry, Michigan State University; (b) Bell Laboratories, Murray Hill; (c) Department of Chemistry, Massachusetts Institute of Technology.
(2) Shah, V. K; Brill, W. J. *Proc. Natl. Acad. Sci. U.S.A.* **1977**, *74*, 3249.
(3) Burgess, B. K.; Jacobs, D. B.; Stiefel, E. I. *Biochim. Biophys. Acta* **1980**, *614*, 196.
(4) Rawlings, J.; Shah, V. K.; Chisnell, J. R.; Brill, W. J.; Zimmermann, R.; Münck, E.; Orme-Johnson, W. H. *J. Biol. Chem.* **1978**, *253*, 1001.
(5) Hoffman, B. M.; Roberts, J. E.; Orme-Johnson, W. H. *J. Am. Chem. Soc.* **1982**, *104*, 860.
(6) Cramer, S. P.; Gillum, W. O.; Hodgson, K. O.; Mortenson, L. E.; Stiefel, E. I.; Chisnell, J. R.; Brill, W. J.; Shah, V. K. *J. Am. Chem. Soc.* **1978**, *100*, 3814.
(7) Cramer, S. P.; Hodgson, K. O.; Gillum, W. O.; Mortenson, L. E. *J. Am. Chem. Soc.* **1978**, *100*, 3398.
(8) Teo, B. K.; Averill, B. A. *Biochem. Biophys. Res. Commun.* **1979**, *88*, 1454.
(9) Wolff, T. E.; Berg, J. M.; Warrick, C.; Hodgson, K. O.; Holm, R. H. *J. Am. Chem. Soc.* **1978**, *100*, 4630.
(10) Armstrong, W. H.; Mascharak, P. K.; Holm, R. H. *Inorg. Chem.* **1982**, *21*, 1699.
(11) Teo, B. K. In "EXAFS Spectroscopy: Techniques and Applications"; Teo, B. K., Joy, D. C., Eds.; Plenum Press: New York, 1981; pp 13–58.
(12) Christou, G.; Hagen, K. S., Holm, R. H. *J. Am. Chem. Soc.* **1982**, *104*, 1744.

0002-7863/82/1504-4703$01.25/0

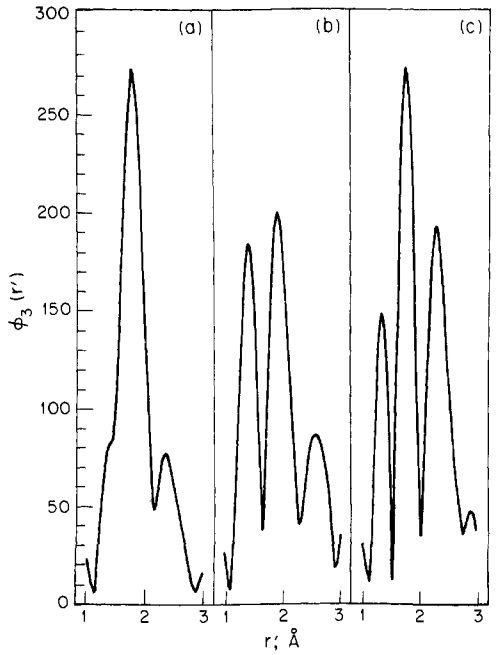

Figure 1. Fourier transforms of the iron K edge EXAFS $k^3\chi(k)$ vs. k of (a) $[(p\text{-}CH_3C_6H_4S)_2FeS_2FeS_2MoS_2]^{3-}$ showing Fe–S and Fe–Fe(Mo) peaks at 1.83 and 2.35 Å (before phase shift correction), (b) $[(C_6H_5O)_2FeS_2MoS_2]^{2-}$ showing Fe–O, Fe–S, and Fe–Mo peaks at 1.40, 1.88, and 2.55 Å (before correction), and (c) the FeMo(co) of nitrogenase, which shows Fe–O(N), Fe–S(Cl), and Fe–Fe(Mo) peaks at 1.33, 1.74, and 2.26 Å (before correction), respectively.

Nitrogenase molybdenum–iron protein (Av1) was purified from *Azotobacter vinelandii*.[3] The FeMo(co) was extracted into *N*-methylformamide (NMF)[2] and brought to a final concentration of 1 mM in iron. This material both displayed the acceptable EPR spectrum of the cofactor[4] (with no evidence for high-spin Fe(III) contaminants) and had the ability to complement the molybdenum–iron protein from *Azotobacter vinelandii UW45*.[2] Samples were loaded anaerobically into polycarbonate holders, frozen, and stored in liquid nitrogen when not in the spectrometer.

Iron K-edge X-ray absorption measurements were made at ca. 160 K with the fluorescence technique at SSRL (see Figure A, supplementary material: Experimental Section).

A comparison of the Fourier transform of the cofactor data with those of model compounds (cf. Figure 1) measured and analyzed in a similar fashion prompted us to assign the three peaks in the cofactor as Fe–O (or N),[13] Fe–S (or Cl), and Fe–Fe (and/or Mo) backscatterings, in order of increasing distance. The Fourier transform of the iron EXAFS spectrum of $[(p\text{-}CH_3C_6H_4S)_2FeS_2FeS_2MoS_2]^{3-}$ (**1**) shows Fe–S and Fe–Fe(Mo) peaks[14] (Figure 1a), and that of the iron EXAFS of $[(C_6H_5O)_2FeS_2MoS_2]^{2-}$ (**2**) shows Fe–O, Fe–S, and Fe–Mo peaks[14b,15] (Figure 1b). Since these peaks are not fully resolved in distance space, they cannot be decomposed into individual contributions via Fourier filtering, and parameter correlations impair the curve-fitting attempts using three- or four-term backscattering models. So that reliable structural information for the cofactor and the model compounds could be obtained, the following iterative procedure was developed: First, the filtered $k^3\chi(k)$ data (filtering window 0.7–4.2 Å) were fit with a two-term model containing only Fe–O and Fe–S contributions (supplementary material, Figure B, dashed curve). The residual from the fit ($k^3\chi_M(k)$) was obtained, Fourier filtered (window 1.6–3.0 Å), and fit with a two-term model containing Fe–Fe and Fe–Mo contributions (supplementary material, Figure C, dashed curve). For a more accurate fit of the Fe–O and Fe–S terms, the Fourier filtered Fe–Fe(Mo) component was subtracted from the total filtered spectrum, leaving a residual spectrum ($k^3\chi_L(k)$) presumably containing only Fe–O and Fe–S contributions, which was again Fourier filtered (window 0.7–3.4 Å) and fit with Fe–O and Fe–S terms (supplementary material, Figure D, dashed curve). The best fit Fe–O, Fe–S, Fe–Fe, and Fe–Mo distances from the two-term fits of $k^3\chi_L(k)$ and $k^3\chi_M(k)$ are listed in Table I, along with the relevant parameters for the two model compounds. A plot of the total filtered EXAFS (solid curve) and the sum of the two best two-term fits (dashed curve) is shown in Figure 2. The accuracy of the Fe–O, Fe–S, Fe–Fe, and Fe–Mo distances (ca. 0.05, 0.01, 0.07, 0.02 Å, respectively) is judged from the model compounds.

In order to determine the coordination numbers of the iron atoms in the FeMo(co), as well as to improve the accuracy of the distances obtained from the best theoretical fits, we applied a new "fine adjustment" method based on model compounds (FABM) to the data.[16] The method involves transferring the change in energy threshold relative to the edge position (ΔE_0^p) and the Debye–Waller factor (σ) obtained for each type of neighboring atom from the models **1** and **2** to the FeMo(co) (see Table I).

The reported number of Fe–O(N) bonds, 2.1, requires some comment. Since $[Fe_4S_4(SPh)_4]^{2-}$[17] has a shoulder at 1.35 Å

Table I. Least-Squares Refined Interatomic Distances (r, Å) and Coordination Numbers (N) with Standard Deviations (in Parentheses) for the FeMo Cofactor of the Nitrogenase Enzyme Isolated from *Azotobacter vinelandii*

		model compounds		FeMo cofactor	
bonds		best fit	diffraction	best fit	FABM
Fe–S	r	2.255 (21)	2.256[a,d]	2.215 (32)	2.247 (20)
	N	4.0 (12)	4	3.9 (17)	3.4 (16)
Fe–Fe	r	2.762 (22)	2.691[a]	2.629 (10)	2.656 (27)
	N	1.0 (3)	1	2.6 (4)	2.3 (9)
Fe–Mo	r	2.804 (34)	2.778[a]	2.837 (21)	2.760 (32)
	N	0.5 (1)	0.5	0.3 (1)	0.4 (1)
Fe–O	r	1.847 (70)	1.897[b,d]	1.873 (29)	1.814 (65)
	N	2.0 (6)	2	2.1 (10)	1.2 (10)[c]

[a] From $[(p\text{-}CH_3C_6H_4S)_2FeS_2FeS_2MoS_2]^{3-}$ (1).[14b] [b] From $[(C_6H_5O)_2FeS_2MoS_2]^{2-}$ (2).[14b] [c] "Background peak" subtracted based on $[Fe_4S_4(SPh)_4]^{2-}$. [d] Average values.

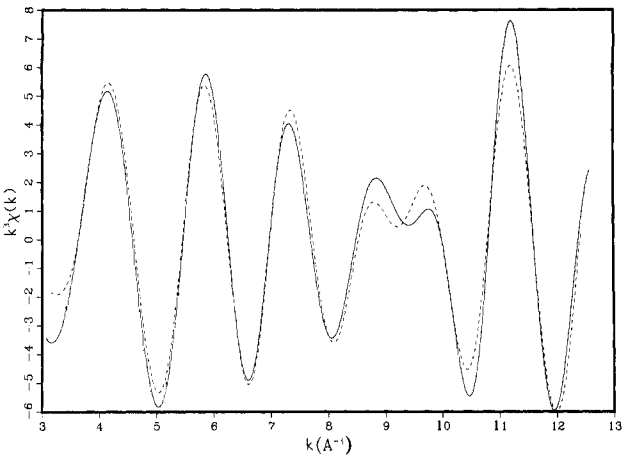

Figure 2. Total Fourier filtered EXAFS, $k^3\chi(k)$ vs. k, spectrum of the FeMo(co) (—) and the sum of the two best two-term fits (---) of $k^3\chi_L(k)$ (with Fe–O and Fe–S terms) and $k^3\chi_M(k)$ (with Fe–Fe and Fe–Mo terms). The individual contribution of each type of scatterer to the total filtered EXAFS, as resolved by our curve-fitting technique, is shown in Figure E, supplementary material.

(13) The amplitude and phase functions for Fe–O and Fe–N backscatterings are similar; here, this peak is analyzed as an Fe–O distance. In Av1 an electron spin echo measurement near $g = 2.01$ shows evidence of a nitrogen atom coupled to the $S = {}^3/_2$ center (W. B. Mims, W. H. Orme-Johnson, unpublished).

(14) (a) Tieckelmann, R. H.; Averill, B. A. *Inorg. Chim. Acta* **1980**, *46*, L35. (b) Teo, B. K.; Antonio, M. R.; Tieckelmann, R. H.; Silvis, H. C.; Averill, B. A., submitted for publication.

(15) Silvis, H. C.; Averill, B. A. *Inorg. Chim. Acta* **1981**, *54*, L57.

(16) Teo, B. K.; Antonio, M. R.; Averill, B. A., submitted for publication.

(before phase-shift correction) in the Fourier transform[18] (due to Fourier truncation and/or residual background), the result obtained for the FeMo(co) (which shows a peak at 1.33 Å, before correction, in the Fourier transform; cf. Figure 1c) may be in error by as much as 50%. If we subtract a "background peak" estimated from $[Fe_4S_4(SPh)_4]^{2-}$, the number of Fe–O bonds reduces to 1.2. Despite these cautions, the data in Table I support the use of the EXAFS of **1** and **2** as good models for the Fe–S(Cl), Fe–Fe(Mo), and Fe–O(N) interactions in the FeMo(co).

In summary, the iron atoms in the FeMo(co) have an average of 3.4 ± 1.6 S(Cl) atoms at 2.25 (2) Å, 2.3 ± 0.9 Fe atoms at 2.66 (3) Å, 0.4 ± 0.1 Mo atoms at 2.76 (3) Å, and 1.2 ± 1.0 O(N) atoms at 1.81 (7) Å as nearest neighbors. The large standard deviation in the number of sulfur and iron atoms may be due to the presence of *different iron sites* with varying number and/or types of sulfur and iron neighbors. Our findings are consistent with (although certainly not limited to) models 4[11] and 5[12] described above. Note that model 4 calls for 3–4 S (or Cl), 2 Fe, 0.3–0.5 Mo, and 1–2 O (or N) neighbors per iron atom, whereas model 5 predicts 4 S, 2.6 Fe, and 0.4 Mo neighbors per iron atom. Finally, it should be cautioned that the structure of the NMF-extracted FeMo(co) from Av1 may be different from the novel cluster in the native enzyme, due to the coordinating power of NMF.

Acknowledgment. We thank Drs. L. S. Powers and B. Chance for generous assistance with the experimental apparatus at SSRL (see supplementary material). This research was supported in part by an NSF grant (8008733 PCM), a USDA/SEA Competitive Research Grant Office grant (5901-0410-8-0175-0), an NIH grant (GM 28636), and by two fellowships (NSF-SPI-7914823 and NIH-GM07294).

Registry No. FeMo(co), 72994-52-6.

Supplementary Material Available: Detailed Experimental Section with five references and five figures, A–E (8 pages). Ordering information is given on any current masthead page.

(17) DePamphilis, B. V.; Averill, B. A.; Herskovitz, T.; Que, L. Jr.; Holm, R. H. *J. Am. Chem. Soc.* **1974**, *96*, 4159.
(18) Antonio, M. R.; Teo, B. K.; Averill, B. A., to be submitted for publication.

Nucleophilic Addition of Phenolate Oxygen to an Unactivated C=C Double Bond

Christopher M. Evans and Anthony J. Kirby*

University Chemical Laboratory
Cambridge CB2 1EW, England

Received April 9, 1982

Under normal conditions ethylene and simple alkyl ethylenes react exclusively with electrophiles: nucleophilic additions are observed only when strongly electron-withdrawing substituents are present. Certain reactions catalyzed by enzymes[1] suggest that this prohibition is not absolute, and we are exploring possible intramolecular additions of oxygen and nitrogen nucleophiles to unactivated C=C double bonds under mild conditions. We have shown[2] that in a suitable system activated by ground-state strain amine nitrogen will add very rapidly to the transannular double bond of an electron-rich stilbene. We now report that phenolate oxygen will add readily to a neighboring monoalkyl ethylene when the groups are brought together in a system exhibiting high effective molarity (EM).[4]

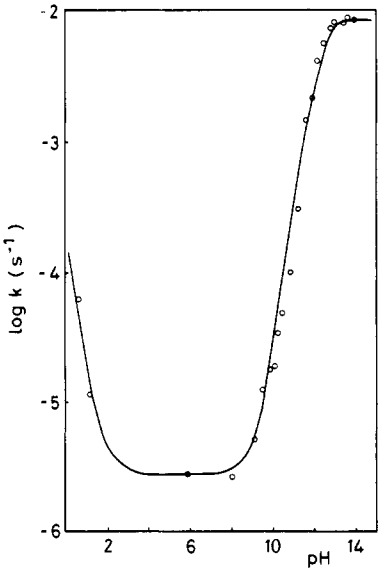

Figure 1. pH profile for the cyclization of **1** → **2** at 39 °C and ionic strength 0.2 M (KCl) in 50% aqueous acetonitrile. The points are experimental; the curve is calculated, by using $k_{H^+} = 2.2 \times 10^{-4}$, $k_0 = 1.8 \times 10^{-6}$ and 8.4×10^{-3} s^{-1}, and pK_a 12.5.

Ganter[5] and Grob[6] and their co-workers have reported relevant cyclizations of several polycyclic olefin–alcohols under basic as well as the more generally favorable acidic conditions. We preferred an olefin–phenol system, which could be converted completely to the phenolate anion and could thus be studied in the absence of complications from the initial ionization step. The key requirement was thus a phenol–olefin that would undergo intramolecular cyclization with a very high EM, and we have prepared several such compounds based on the "trialkyl lock" system of Milstien and Cohen.[7]

The most reactive of these is the phenol–olefin **1** (prepared from

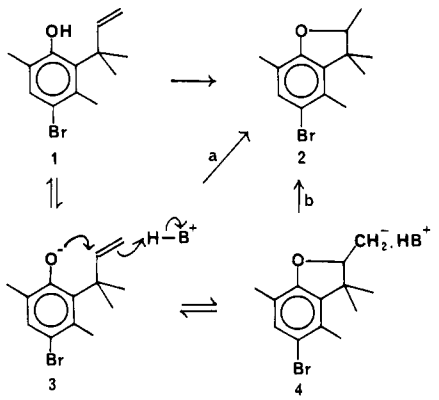

the lactone A[7] by the route shown in eq 1, with the following reagents: (i) Dibal-H; (ii) $(COOH)_2$ in PhMe; (iii) Br_2/CCl_4; (iv) H_2O/THF; (v) $Et_3SiH/BF_3{\cdot}OEt_2$; (vi) Zn/95% EtOH. Both **1** and its cyclization product **2** have been fully characterized spectroscopically). **1** cyclizes to **2** very slowly at neutral or acidic pH, but reaction is rapid above pH 10, and the half-life of the anion is 82 s at 39 °C. The pH–rate profile (Figure 1) shows pH-independent regions from pH 2.5 to 8.5 and above 13, and

(1) Of particular interest are those amino acid ammonia lyases which are reversible and can thus catalyze the addition of ammonia to double bonds without assistance from electron-withdrawing substituents,[2] and oleate hydratase (EC 4.2.1.53), which catalyses the stereospecific hydration of oleic acid to 10-hydroxy stearate.[3]
(2) A. J. Kirby and C. J. Logan, *J. Chem.* Soc., *Perkin Trans. 2*, 642 (1978).
(3) W. G. Niehaus, A. Kisic, A. Torkelson, D. J. Bednarczyk, and G. J. Schroepfer, *J. Biol. Chem.*, **245**, 3790 (1970).
(4) A. J. Kirby, *Adv. Phys. Org. Chem.*, **17**, 183 (1980).
(5) G. M. Ramos Tombo, R. A. Pfund, and C. Ganter, *Helv. Chim. Acta*, **64**, 813 (1981).
(6) G. A. Grob and H. Katayama, *Helv. Chim. Acta*, **60**, 1890 (1977).
(7) S. Milstien and L. A. Cohen, *J. Am.* Chem. *Soc.*, **94**, 9158 (1972). Although these compounds have been shown recently to be less reactive than originally thought,[8] they still show EM's of more than 10^{11} M.[4]
(8) M. Caswell and G. L. Schmir, *J. Am. Chem. Soc.*, **102**, 4815 (1980).

0002-7863/82/1504-4705$01.25/0